

Electron field emission from Ar⁺ ion-treated thick-film carbon paste

Gillian A.M. Reynolds, Lap-Tak Cheng, Robert Bouchard, Paul Moffett, Howard Jones, and Linda F. Robinson

DuPont Central Research and Development, Wilmington, Delaware 19880

S. Ismat Shah

Department of Materials Science and Engineering and Department of Physics and Astronomy, University of Delaware, Newark, Delaware 19716

Daniel I. Amey

DuPont Electronic Technologies, Research Triangle Park, North Carolina 27709

(Received 14 January 2002; accepted 11 July 2002)

Ion bombardment was used to produce electron-emitting microscale features on surfaces of thick films printed with carbon pastes. This technology can potentially enable the development of large-area field emission displays. Systematic investigations using microscopy and electron field emission experiments have demonstrated a close link among paste formulation, ion processing parameters, and the development of surface microstructures. These investigations were also useful in understanding the fundamentals of microstructure formation under ion bombardment and the field emission characteristics of the carbon-based emitters. Several device concepts aimed toward achieving a low-voltage switchable triode were also tested with varying degrees of success. In this paper, we discuss various technological issues related to the materials, processes, and devices.

I. INTRODUCTION

There is intense research underway to develop vacuum electronics and flat panel displays based on field emission. The original idea, as presented by Spindt,¹ involved Si microtips. The creation of Spindt tip field emitters requires several lithographic steps, and not only are the resulting tips susceptible to mechanical damage but they can be easily contaminated by exposure to the atmosphere. These sensitivities require fabrication and particularly operating pressures better than 1×10^{-6} torr. The current field emissive material of choice is carbon in a variety of forms including, for example, graphite, carbon nanotubes, diamond, and various mixtures thereof.²⁻⁵

Several techniques have been used to create the nanostructures associated with these carbon-based field emitters. These include chemical vapor deposition,^{6,7} pulsed laser deposition,^{8,9} epoxy mixing,¹⁰ etc. Structures are also known to form on a variety of surfaces as a result of ion bombardment. These structures take the form of cones, hills, or whiskers. Feature formation has been observed on ion bombarded metal surfaces that have been seeded with another type of metal.¹¹ Ion bombardment of carbon surfaces has also been shown to produce conelike features and carbon nanostructures such as nanotubes.¹²⁻¹⁵

In this paper, we discuss the formation of cones from a thick-paste graphite film upon exposure to Ar⁺ ions. The cones formed as a result of the ion bombardment are

on the order of several microns in length and exhibit electron emissive properties under an external electric field. The effects of such parameters as ion bombardment time, substrate temperature, and oxygen exposure on the morphology and resulting emission are also discussed.

II. EXPERIMENTAL

The conelike features and resulting electron emitters were fabricated using a two-step process of screen-printing and Ar⁺ ion bombardment of thick-film carbon paste materials. The screen-printed samples were derived from paste mixtures of inorganic powders (including carbon-based powders like graphite and carbon black), organic polymers, solvents, and surfactants. The inorganic powders contained a relatively low melting glass to ensure sintering of the composite and adherence to the substrate. A standard paste composition of 50/50 by weight inorganic to glass was used in this work. The simplest emitter structure made was a diode. In this configuration, a 1-mm-thick and 2.5-cm-square soda-lime glass was used as a substrate. A silver layer was screen-printed onto the glass substrate and pre-fired at 525 °C to form a 6–7- μm -thick electrode. The carbon paste was then screen-printed on top of the silver electrode to a thickness of 10–20 μm and fired at 475 °C in air. The

firing removed all the organic constituents of the paste material and left behind only the inorganic layer. The samples were then subjected to an Argon plasma using an 8-cm Kaufman source. During the ion bombardment, the samples were covered with a graphite mask in order to expose only a 12×12 mm (approximately 1 cm^2) area to the ions. Typically, samples were positioned at either a 90° or 45° angle to the incoming ion beam and treated under 1.5×10^{-4} torr of argon pressure for 30 min at 1200-eV beam energy, 120-mA beam current, approximately 2-mA/cm^2 current density, and 40-V discharge voltage under total beam neutralization conditions. A heating stage was built into the system which allowed control over the substrate temperature (T_S) during ion bombardment. Values for T_S could be varied from 100 to 450°C . Generally, without temperature control, T_S reached approximately 350°C during ion bombardment. Active cooling of the substrate was needed to keep the

temperature at 100°C . After ion bombardment, emission currents from the 1-cm^2 exposed areas were measured in a diode configuration with the ion-treated graphite paste acting as the cathode and an indium tin oxide (ITO) coated phosphor screen acting as the anode. The diodes were operated at 1×10^{-6} torr by applying pulsed negative voltages to the cathode at duty cycles in the range of approximately 0.02% to approximately 1% (pulse widths of 3 to $40 \mu\text{s}$ and frequencies of 60 to 100 Hz). For the diode configuration, the cathode-anode spacing was on the order of 1 to 1.25 mm.

The sample morphologies were studied using scanning electron microscopy (SEM) and transmission electron microscopy (TEM). For SEM [Hitachi S-800 field-emission scanning electron microscopy (FE-SEM, Mito City, Japan)], imaging was performed at 4-kV accelerating voltage at a 15-mm working distance and 2500 magnification. The features produced on the samples' surface

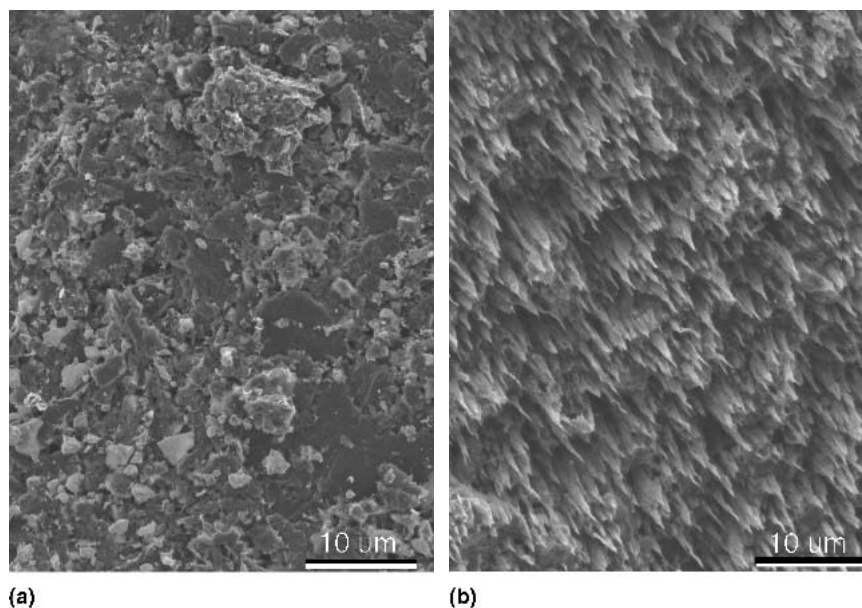


FIG. 1. Morphology (a) before and (b) after etching for 30 min in 1200-eV argon ion. The morphology consists of cones of approximately $3 \mu\text{m}$ in height. Features form in the direction of the incident ion beam.

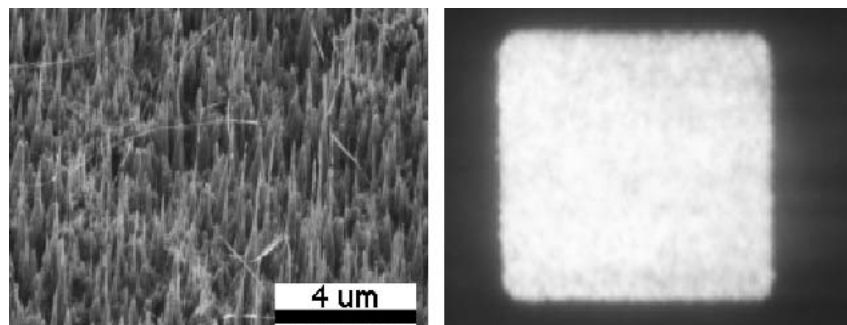


FIG. 2. SEM and pulsed diode field emission (1.44-cm^2 emissive area) of an etched graphite paste sample ($3 \mu\text{s}$, 60 Hz). The morphology consists of whiskers supported by cones of approximately $2 \mu\text{m}$ in height. Features form in the direction of the incident ion beam.

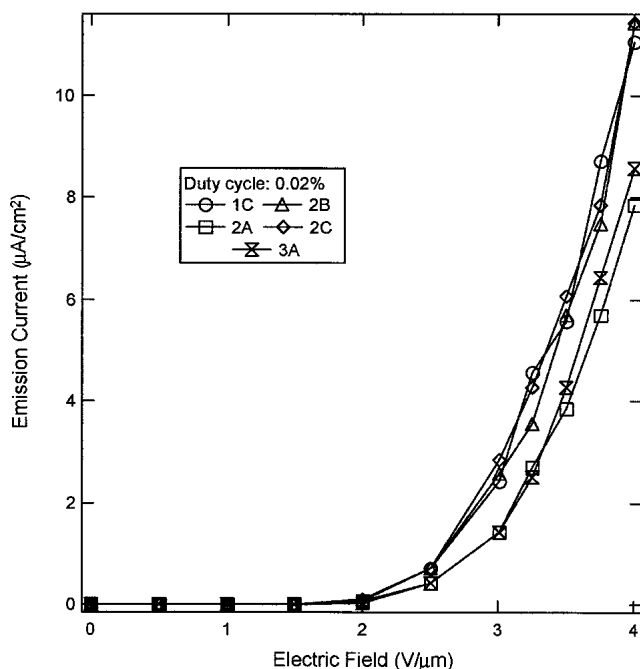


FIG. 3. I - V curves (duty cycle approximately 0.02%) from samples treated with an Ar⁺ ion beam under similar conditions (1200 eV, 120 mA, 45 min) at a substrate temperature of 450 °C.

by ion bombardment were evaluated further by high-resolution transmission electron microscopy (HRTEM) (Philips CM-20 TEM, Eindhoven, The Netherlands) using an accelerating voltage of 200 kV. To achieve this, surface layers of the ion beam etched carbon were gently scraped using clean razor blades. The scraped material was deposited directly onto perforated carbon films supported on 3-mm TEM Cu grids.

III. RESULTS AND DISCUSSION

A. Mechanisms of, and factors affecting, morphology formation

Figures 1(a) and 1(b) are SEM images of the morphology of the screen-printed carbon paste before and after Ar⁺ ion bombardment, respectively. Before bombardment, the morphology is inhomogeneous, with flakes of glass frit and graphite visible on the surface as light and dark regions, respectively. These untreated films exhibit no electron emission. After ion bombardment, the morphology consists of whiskers, when visible, supported by larger triangular-shaped cones. The cones, which form in the direction of the ion beam, are on the order of 2 to 4 μm in height, while whiskers can be tens of microns long. Figure 2 shows the cone morphology (SEM) and some of the earliest emission results from these structures. The emission is from a 2.5-cm-square sample

(effective emissive area 1.44 cm²) running at 0.02% duty cycle with a current density of 4.5 μA/cm² at 3 V/μm. Figure 3 shows the reproducibility of the I - V curves for five samples running at approximately 0.02% duty cycle and etched under similar conditions for 45 minutes. The turn-on field is in the range of 1.5–2 V/μm, with a current density of approximately 5 μA/cm² at 3.5 V/μm. These turn-on voltages are comparable to carbon nanotube devices in the literature. The direct current (dc)-equivalent current densities are higher than some carbon nanotube diode devices cited in the literature.^{2,16} Using a 1-megapixel camera to expand the emission from a 1 × 1 cm area, emission spots were not distinguishable, suggesting emission site densities on the order of 10⁴ to 10⁵ sites/cm². This estimate is reasonable when compared to site densities obtained via scanning anode field emission microscopy in the literature.¹⁷

The microstructure of the whiskers and cones was studied by high-resolution TEM. Figure 4 shows the HRTEM of a cone with a whisker extending from the tip of the cone. The whisker is generally amorphous while the supporting cone has an ordered outer layer (approximately 10-nm wide) covering an amorphous interior. The ordered outer shell on the cone consists of graphene planes which are oriented perpendicular to the cone growth direction. Generally, in a carbon filter, graphene planes grow parallel to the fiber growth direction. This microstructure could point to regrowth as a possible mechanism for the cone structure formation.

The cones form as a result of the surface chemical or morphological inhomogeneities. Carbon has a very low sputter yield.¹⁸ The glass frit around the carbon-rich area sputters at a higher rate leaving behind carbon regions that, under anisotropic etching, form conical shaped regions. The orientation of the cones in the direction of the ion beam also supports the preferential etching process as a possible mechanism for cone formation. In this case, the physical etching generated by ion impact defines the direction of cone growth by effectively eroding cones that are growing off angle to the ion trajectory. This results in the cones always growing, as observed, in the direction of the ion beam. On the other hand, the growth of whiskers, which are several microns in length, could not be explained solely on the basis of preferential sputtering. A simultaneous growth process has to occur. Also, the presence of the oriented crystalline outer layer (Fig. 4) cannot be explained as due purely to a sputter-etching process. Most likely, cone and whisker dimensions stem from a combination of etching and regrowth processes. Thus, the physical etching, due to preferential sputtering, defines the orientation and shape of the cones and a concurrent surface atom migration and vapor-phase redeposition of sputtered carbon assists in whisker formation. To further study the cone formation process, ion bombardment was performed as a

function of time by treating samples for 15 to 45 min under similar ion source conditions. Figure 5 shows the resulting morphologies. For times as short as 15 min [Fig. 5(a)], the inhomogeneous surface becomes pitted and acts as nucleation sites for the emergent short cones that are visible. As the ion bombardment time increases to 30 and 45 min [Figs. 5(b) and 5(c), respectively], the overall surface morphology remains inhomogeneous while the cone densities and cone aspect ratios increase.

The overall morphology of the ion-bombarded graphite paste material is fairly inhomogeneous. Cone heights, thickness, separations, and radii of curvature vary within and between samples. An ideal morphology would be one in which all the cones were uniform in structure and height with an even distribution over the emitting surface. The ability to control the morphology to this degree would result in an emitter where the majority of the sites contributed to the emission process. If the variations in

cone density or height could be changed by external parameters, the system could be tailored to the desired emission. To determine the extent to which the ion-treated graphite paste morphology and resulting device emission could be controlled, experiments were conducted to study the effects of contaminants, substrate temperature, and ion bombardment time on the properties.

We have found that cone formation is possible on a variety of carbon surfaces such as graphite and carbon black. However, the presence of contaminants (i.e., non-graphitic components) can destroy cone formation. Figure 6 shows the microstructure of variable width stripes of graphite and glass frit (50/50 by weight) printed on a pure glass background. Here the glass acts as the contaminant. As the stripe width is decreased from 2 mm to 254 μm , the degradation in cone formation is clearly evident. Since the sputtering yield of low melting oxide is much higher than that of carbon, for every carbon atom

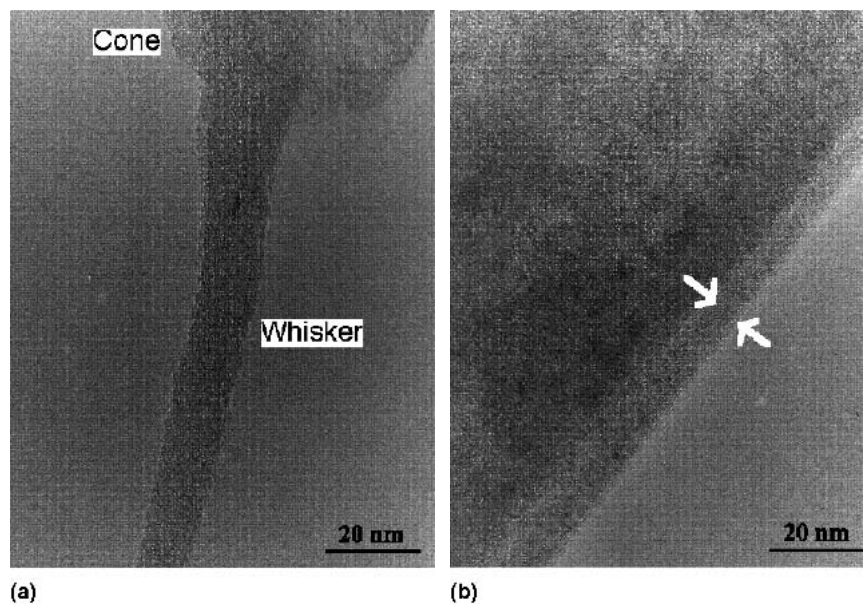


FIG. 4. (a) High-resolution TEM of a whisker and cone. (b) Extent of the ordered outer layer of the cone (approximately 10-nm wide), as indicated by the arrows.

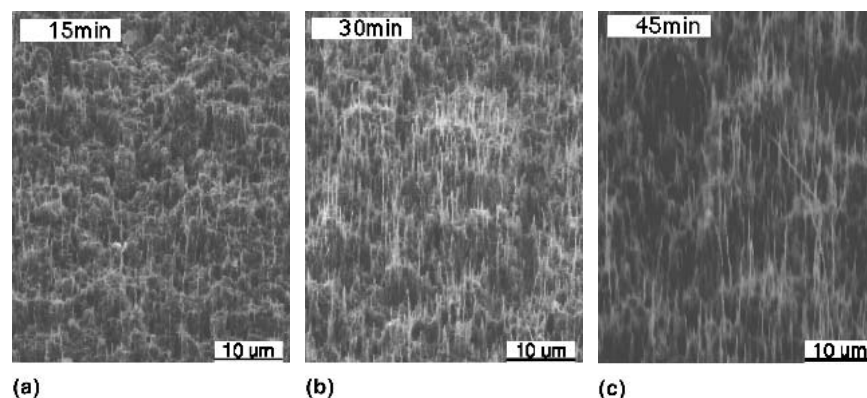


FIG. 5. Showing the effects of Ar⁺ ion bombardment time on morphology. Samples were treated under similar conditions for (a) 15, (b) 30, and (c) 45 min.

removed by ion etching, five or more oxygen atoms are generated. This source of reactive oxygen represents an isotropic chemical etching process that competes effectively with the anisotropic physical etching of ion bombardment. Chemical etching tends to round off any sharp

features and seed cones, thus decreasing cone density and sharpness. As the ratio of exposed oxide/carbon surface area increases, cone formation deteriorates rapidly. Also, the excess glass, during ion bombardment, recondenses on the cone surface, as shown in the high-resolution

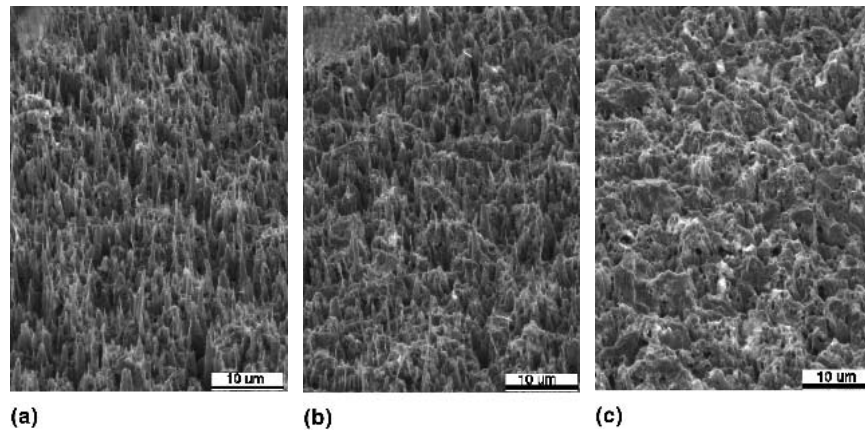


FIG. 6. Degradation in cone formation with decreasing graphite paste stripe width. Graphite paste stripe width of (a) 2 mm, (b) 762 μm , and (c) 254 μm .

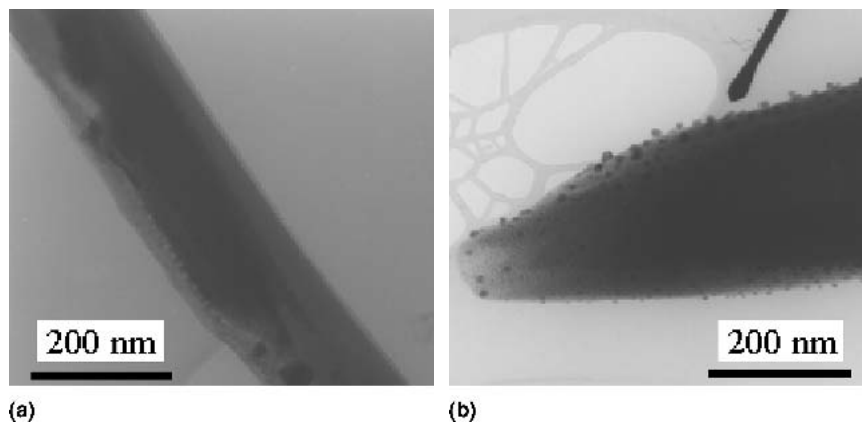


FIG. 7. High-resolution TEM of cones created from (a) an all-graphite paste surface and (b) a graphite surface near a pure oxide edge.

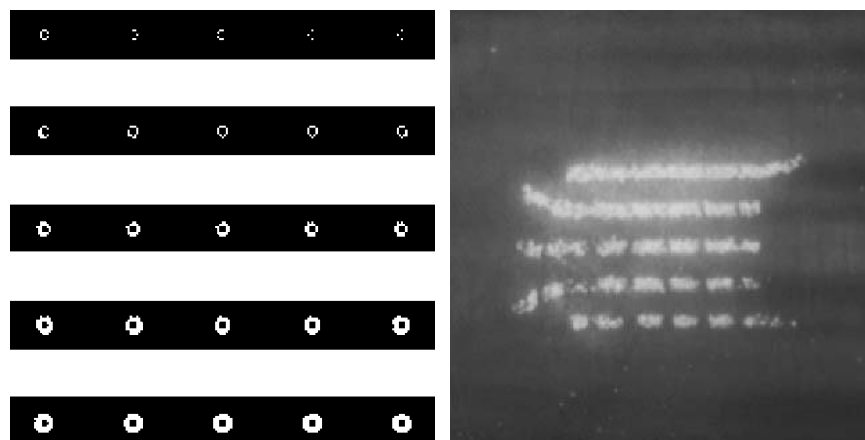


FIG. 8. Effects of contaminants on emission. The emission improves with decreasing amount of dielectric contaminant (bottom to top). Black regions represent graphite, and white regions, dielectric.

TEM of Fig. 7(b). This HRTEM image is compared to an all graphite paste cone surface, Fig. 7(a). In the all graphite paste, the cone surface is free of a glass coating. We have observed that surfaces such as those in Fig. 7(b) will not emit as efficiently as those in Fig. 7(a). This contamination effect is shown in Fig. 8, which consists of a sample with 25–127 μm of exposed rings of dielectric (white regions) surrounding graphite (black regions). For the lines with large areas of exposed dielectric (contaminant), after ion bombardment, emission is absent from the graphite holes. Emission occurs in the etched graphite line in regions far enough away from the exposed dielectric. The emitting line becomes more continuous as the amount of exposed dielectric and its influence on morphology contamination are reduced.

B. Device characterization

The electron field emission properties of the ion treated surfaces and the overall performance of the diodes made from these samples were characterized by operating devices in a pulsed mode. In general, emission from the ion-treated thick-film samples does not deteriorate after exposure to atmosphere. However, physical contact with the ion-treated surface can cause damage to the microstructure and the resulting emission. The emitters can be operated at moderate vacuum at pressures on the order of 1×10^{-5} torr, two orders of magnitude higher in background pressure than that required by traditional

Spindt tips. An ion-treated sample can also tolerate repeated exposure to atmosphere without any observable degradation in the emission properties.

We have studied the effects of substrate temperature, T_s , during ion bombardment on the morphology and emission. The results in Fig. 9 show the diode pulsed emission from samples ion treated at $T_s = 100, 200, 300,$ and 450 $^{\circ}\text{C}$. There is an increase in emission current and uniformity with increasing T_s . There are no distinct differences in the morphologies at the SEM level in samples treated at different temperatures. It is possible that the cone structures are becoming more graphitic in the outer layer with an increase in temperature. The state of the graphitic outer layer within the cones created in these experiments is yet to be analyzed via HRTEM.

Tests done on many ion-treated samples have shown phenomena such as the existence of a distribution of emitter threshold voltages. In pulsed diode mode, as the anode voltage is increased, emitters turn on according to their relative work function characteristics. The emitters generally remain turned on for about $2 \text{ V}/\mu\text{m}$ beyond their threshold voltage. After this point the population of emitters with lower threshold burn out. This burnout is often accompanied by arc discharge at hot spots on the sample which are associated with high current. Figure 10 shows the I - V data for a diode device for two voltage ramps. On the first voltage ramp, the low turn-on emitters burn out which results in a higher turn-on voltage for the second voltage ramp. As long as the burn-out voltage is

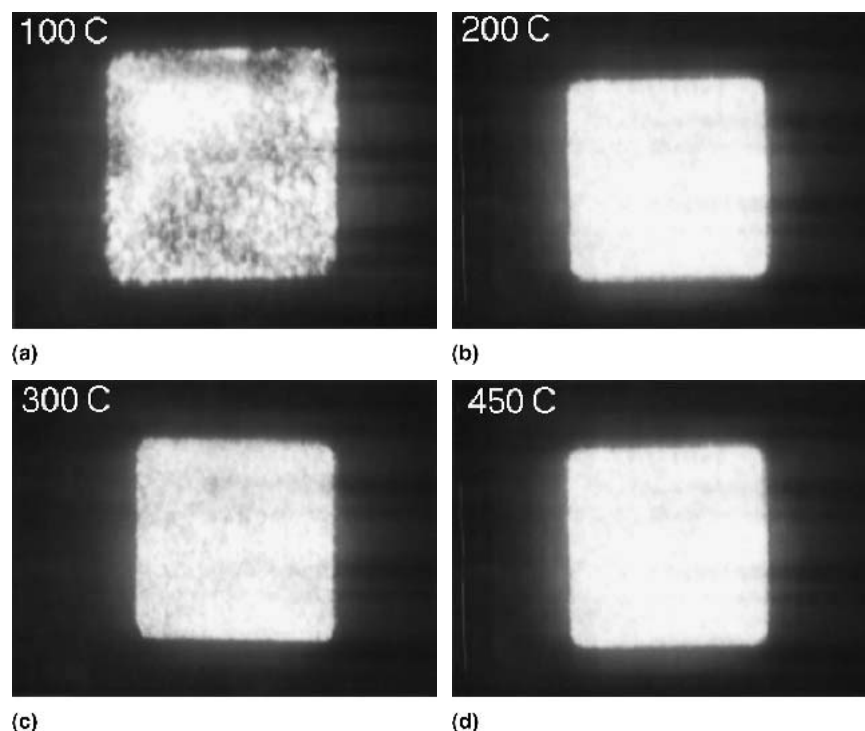


FIG. 9. Pulsed emission (duty cycle approximately 0.02%) from samples (1.44-cm^2 emissive area) that were Ar⁺ ion treated with substrate temperatures, T_s , of (a) 100 $^{\circ}\text{C}$, (b) 200 $^{\circ}\text{C}$, (c) 300 $^{\circ}\text{C}$, and (d) 450 $^{\circ}\text{C}$.

not exceeded for the low turn-on emitters, the emission characteristics of the samples can be retraced on subsequent voltage ramps.

Field emission lifetime studies have also been performed on the diode emitter devices. When the emitters are driven at high duty cycle (>5%) and with high electric fields, accelerated degradation of emission sites and emission uniformity have been observed. However, when the duty-cycle and drive field are maintained below these limits, emission currents remained stable for several hundred hours of operation. Figure 11 shows the lifetime tests of a diode device with a copper anode operating constantly at 4 kV at a duty cycle of 0.8% (40- μ s pulse, 200 Hz). These parameters represent a high stress test for the emitters, corresponding to about 30 times the typical display end use duty cycle at peak voltage and about 15,000 h of run time.

The feasibility of the emitters to perform as true field emission devices was determined by fabricating a simple wire-gate triode system. This design separates the triode structure into two subassemblies: the cathode, containing graphite emissive elements, and a wire gate electrode. A 1 \times 1 cm all graphite surface was ion treated to develop surface structures and was used as the cathode. The sample was checked for diode emission. A 127- μ m-thick polyimide tape was placed on two parallel edges of the glass substrate to serve as stand-offs. Wire of 64- μ m diameter and coated with 2 μ m of varnish was wound onto the glass substrate to serve as the gate electrode. A phosphor-coated ITO glass was used as the anode with a cathode to anode spacing of 2 mm. The cathode was connected to a pulsed negative voltage power supply, and the gate wire and anode were connected to earth ground (via an electrometer) and to a positive-dc high voltage power supply, respectively. The onset of background emission was measured to be 4.5 kV. To keep the emitters in the off state, the anode voltage, V_A , was kept at

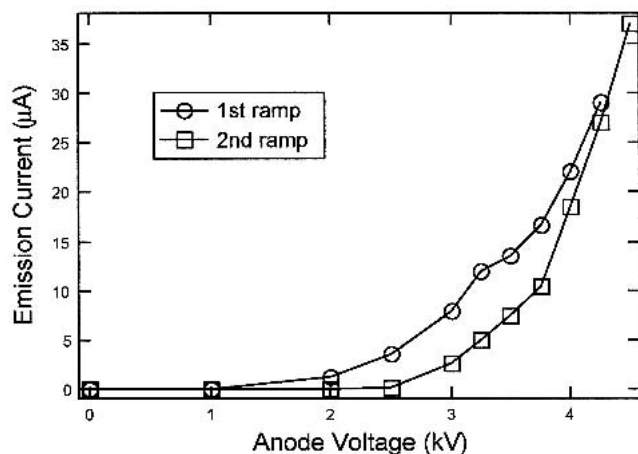


FIG. 10. How the population density decrease on a second voltage ramp leads to higher turn-on fields.

4 kV. Triode switching in the form of bright lines against a dark background was observed at cathode voltages (V_C) as low as -300 V (Fig. 12). At -400 V, an emission current of about 14 μ A was measured at 2% duty cycle.

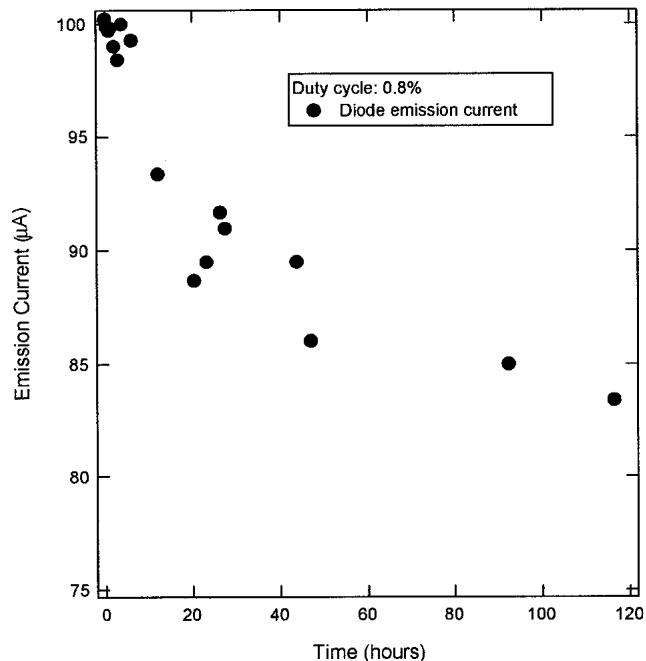


FIG. 11. Emission current as a function of time for a diode device run at 4 kV and 0.8% duty cycle and at pressures of 1×10^{-6} torr.

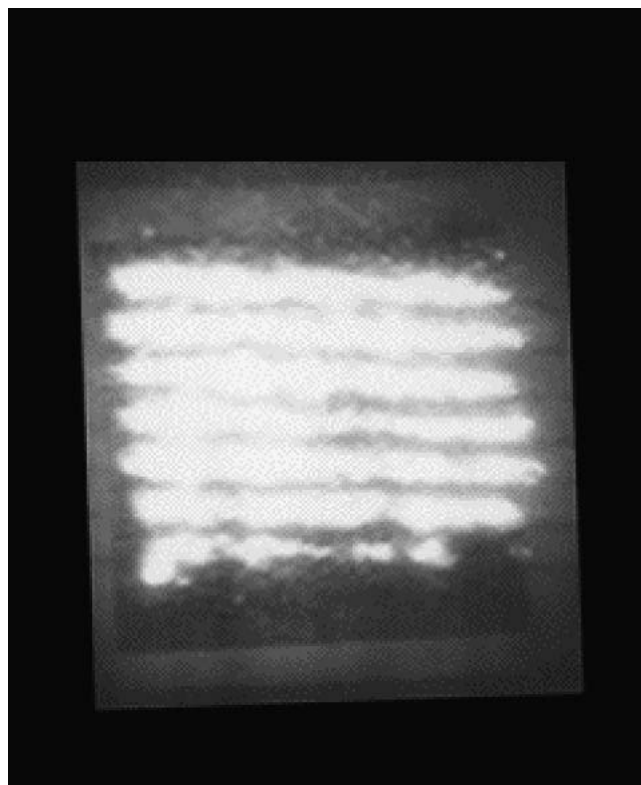


FIG. 12. Triode emission from a 7-wire sample.

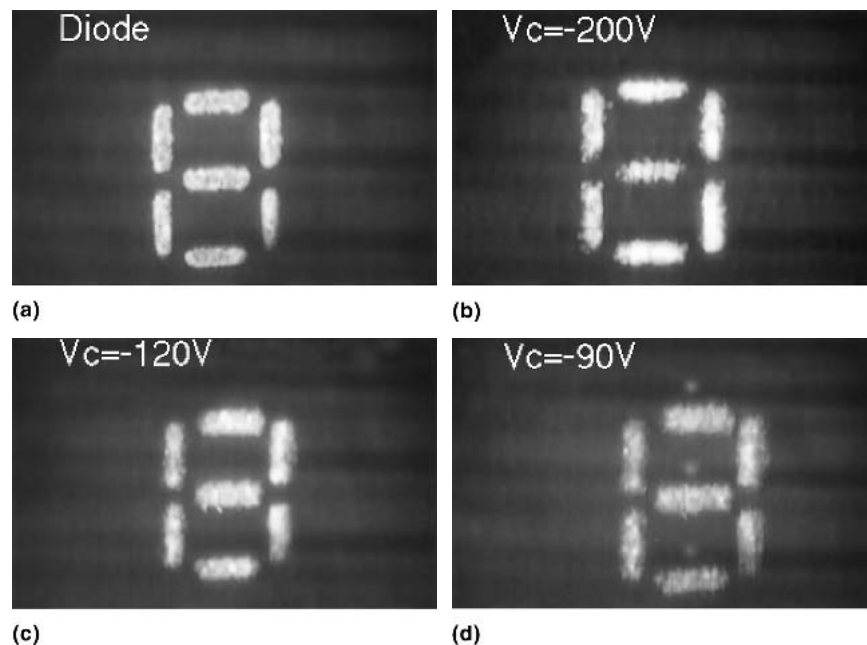


FIG. 13. (a) Diode emission and triode emission from a 7-segment display operating at 20 μ s and 60 Hz with (b) 127- μ m gate to cathode spacing with $V_C = -200$ V and $V_G = 120$ V, (c) 51- μ m gate to cathode spacing with $V_C = -120$ V and $V_G = 30$ V, and (d) 51- μ m gate to cathode spacing with $V_C = -90$ V and $V_G = 60$ V.

To further study the wire gate triode concept, a 7-segment alphanumeric cathode was also fabricated. A wire-gate electrode was made with the gate to cathode spacing defined by the thickness of the polymer film spacer used, as described above. A 7-terminal relay was built to facilitate the individual operation of each segment on the cathode. The cathode was connected to a pulsed negative voltage power supply, while the anode was connected to a positive-dc high voltage power supply. The anode to cathode spacing was 2.75 mm. To reduce the switching voltage required at the cathode, the gate was biased with a positive voltage, V_G . Figure 13 shows the triode performance of this device at three cathode to gate spacings. As this spacing was decreased from 127 to approximately 51 μ m, V_C decreased from -300 to -90 V, thus demonstrating sub-100-V switching of a field emission display (FED) triode device fabricated with graphite thick-film paste technology. The segmented device shows good contrast, stable operation, and minimal image spreading despite the cathode to anode spacing. Improvements need to be made with respect to the uniformity of the segments and poor image edge definition.

IV. CONCLUSIONS

We have created an electron field emitter by using ion bombardment to transform the morphology of screen-printed graphite thick-film pastes. Adequate emitter site density and uniformity, high brightness, and contrast at

low anode voltages are achievable with this emitter material technology. Aging studies of up to several hundred hours at 30 times application duty cycle also demonstrated considerable emitter durability. Using a wire-gated concept, triode operation with sub-100-V switching was observed.

ACKNOWLEDGMENTS

The authors particularly thank Gail Raty for her work with the SEM images. We also acknowledge the help of Dr. S. Subramoney (HRTEM), A. West, B. Farquhar, and S. Harvey.

REFERENCES

1. C.A. Spindt, I. Brodie, L. Humphrey, and E.R. Westerberg, *J. Appl. Phys.* **47**, 5248 (1976).
2. F. Ito, K. Konuma, and A. Okamoto, *J. Appl. Phys.* **89**, 8141 (2001).
3. W.A. de Heer, A. Chatelain, and D. Ugarte, *Science* **270**, 1179 (1995).
4. V.I. Merkulov, D.H. Lowndes, and L.R. Baylor, *Appl. Phys. Lett.* **75**, 1228 (1999).
5. D. Zhou, A.R. Krauss, T.D. Corrigan, T.G. McCauley, R.P.H. Chang, and D.M. Gruen, *J. Electrochem. Soc.* **144**, 224 (1997).
6. C. Wang, A. Garcia, D.C. Ingram, M. Lake, and M.E. Kordesh, *Electron. Lett.* **27**, 1459 (1991).
7. W. Zhu, C.P. Kochanaski, S. Jin, and L. Seibles, *J. Appl. Phys.* **78**, 2707 (1995).
8. A.A. Voevodin and M.S. Donley, *Surf. Coat. Technol.* **82**, 199 (1996).
9. G.T. Visscher, D.C. Nesting, J.V. Badding, and P.A. Bianconi, *Science* **260**, 1496 (1993).

10. P.G. Collins and Z. Zettl, *Phys. Rev. B* **55**, 9391 (1997).
11. G.K. Wehner, *J. Vac. Sci. Technol., A* **3**(4), 1821 (1985).
12. J.A. Floro, S.M. Rossnagel, and R.S. Robinson, *J. Vac. Sci. Technol. A* **1**, 1398 (1983).
13. Z. Wang, F. Zhu, W. Wang, G. Yu, and M. Ruan, *Appl. Phys. A* **71**, 353 (2000).
14. J.A. Van Vechten, W. Solberg, P.E. Batson, J.J. Cuomo, and S.M. Rossnagel, *J. Cryst. Growth* **82**, 289 (1987).
15. W.A. Solberg and I.L. Spain, *J. Vac. Sci. Technol. A* **8**, 3907 (1990).
16. K.H. Park, K.M. Lee, S. Choi, S. Lee, and K.H. Koh, *J. Vac. Sci. Technol. B* **19**, 946 (2001).
17. L. Nilsson, O. Groening, P. Groening, O. Kuettel, and L. Schlapbach, *J. Appl. Phys.* **90**, 768 (2001).
18. S. Ismat Shah, in *Handbook of Thin Film Process Technology*, edited by S. Ismat Shah and D. Glocker (IOP, Bristol, U.K., 1995).